Study of Facial Skin and Aural Temperature

BY EDDIE Y.K. NG, WIRYANI MULJO, AND B. STEPHEN WONG

Using Infrared Imagers With and Without Temperature Reference Source

This article aims to study the correlations between the facial skin surface and contact aural temperatures using two types of infrared (IR) scanners: 1) imager with external temperature reference source (TRS) to set the threshold temperature (no actual reading but with color display mode only) and 2) imager with direct threshold temperature setting, which can be used for all type of operations (with skin temperature reading). To mimic the real situation at checkpoints such as air- and seaports, control screening and data analysis on 30 subjects with three known conditions for an intervenient time using a Type 2 scanner were investigated. The noncontact ear temperature was more closely related to contact-measured aural reading after running, drinking a hot beverage, and under normal conditions. Next, the results based on 750 blind sample sizes obtained by the Type 1 scanner are vital in determining two very important pieces of information: the best (yet practical) region on the face to analyze the suggested procedure to achieve an optimal preset threshold temperature for the Type 1 imager since that type is widely used.

Human body temperature undergoes only slight variations in a course of a person's lifetime. Variations of the body temperature may be due to fever, exertion, and extremely high or low environmental temperatures. A sudden infectious disease outbreak that began in mid-March 2003, popularly known as *severe acute respiratory syndrome* (SARS), and the avian flu are highly contagious and deadly diseases [1], [2]. A SARS-infected patient usually undergoes fever approximately ten days after the day of infection; similarly, the symptoms of bird flu are fever and cough. The outbreak has ignited studies and research (and even the general public interest) in the field of IR imaging system [5].

Based on Stefan-Boltzmann Law, all objects are continually emitting radiation at a rate and with a wavelength distribution that depends on the temperature of the object and its spectral emissivity, $\varepsilon(\lambda)$ [6]–[8]. An IR scanner system is a device that captures IR energy that emits a short wavelength invisible to the human eye and converts it to electric voltage or current signal. The signal is then displayed in a pattern that is visible to the human eye [6]. In the field of IR thermography, *blackbody* is defined as an object that absorbs all radiation energy that impinges on it and, conversely, is a perfect radiator, $\varepsilon = 1$. In fact, real objects are all nonblackbody emitters due to the following three factors: energy absorptance, energy transmittance, and energy reflectance. These factors are highly dependent on the nature of the object, such as its temperature and emissivity. Several external parameters, such as transmittance of the air, ambient temperature, humidity, and distance also affect the accuracy of

> **H**uman body temperature undergoes only slight variations in a course of a person's lifetime.

thermal camera. The emissivity of clean, dry human skin is close to the emissivity of blackbody, $\varepsilon = 0.98$. The actual value of the emissivity of particular area in a human face may depend on face contour, makeup (cosmetics), sweat, and skin complexion.

Thermal imagers available in the market during the SARS outbreak in 2003 can be broadly divided into four different types [7], [13], [14]: 1) thermal imager system (TIS) without any temperature indication but with external TRS, 2) TIS with skin temperature indication and internal TRS, 3) TIS with skin temperature indication defined by external TRS, 4) TIS with body temperature indication defined by an external TRS and a temporal thermometer. TIS offers much promise to be used as a fast, blind mass-screening device to detect potential SARS or bird flu patients. Large effort has hitherto been put to examine the correlation between IR imaging temperature readings and deep body temperature values for the Type 2 imager [5], [6], whereas Types 3 and 4 were reported in the press but have yet to be used widely. Also, there are efforts to minimize the differences and to find alternative solutions to screen out suspected SARS or avian flu patients. This article aims to study the aforesaid correlations using the first two types of scanners. The data for patients entering a hospital would be very different than data for passengers walking through aerobridges in airports. Air motion, ambient temperature, perspiration (e.g., from hand luggage), glasses, physical strain, alcohol, a hot beverage, cosmetics, immediate past history of the face, or even deliberate cooling of the face are just few of such variables. Control screening and data analysis on subjects with three known conditions (well rested, after a hot drink, and after running) are thus investigated.

Materials and Methods

Apparatus
➤ Braun digital tympanic thermometers
➤ Mercury thermometers
➤ IRTRS (IR system operated at a hospital with three blackbody calibrators or TRS) [9]
➤ Set of computers
➤ Strip thermometers
➤ ThermalVision900 [10]

Materials
➤ Hot tea

Software
➤ ImageTool
➤ ImageJ
➤ Microsoft Excel

Systems Description
The study was basically conducted by performing two major temperature measurements taken by two systems: 1) IRTRS with only color display mode and 2) ThermalVision900 (TVS900) with direct temperature readings. The IRTRS screens and captures color images and saves them as a black to white range of color displays. Darker colors represent lower temperatures, and lighter colors represent higher temperatures. The IRTRS used three blackbody calibrators, which serve as reference sources of the system. Each of the blackbodies was set to emit radiation at constant temperatures of 32 °C, 35.1 °C, and 37 °C. The TVS900 on the other hand, has its own blackbody reference located within the scanner. The system is able to display and save color images. The system allows the object parameters setting to be varied [emissivity, ambient and atmosphere temperatures, object distance, transmittance, and relative humidity (RH)]. It is also able to measure the temperature of any points or areas of the image captured. Thus, it offers flexibility for the user to determine temperatures at various sites as compared to the IRTRS. The system comes together with a set of lenses for temperature taking at different distances.

Procedures of Data Collection

IRTRS (No Temperature Reading but with Color Display Only)
The system was set up in an indoor nonairconditioned passageway. Blackbody calibrators and a computer monitor (to store images) were set in line with a yellow box on the ground where the hospital staff and visitors stood when images were captured. The thermal camera itself was planted in the ceiling, and it was 4.5 m above the yellow box. Hospital staff were stopped, and their tympanic temperatures of both ears were taken. After that, they were asked to look straight ahead for their images to be captured. The samples were taken randomly (the subjects might be the same but at different times). Ambient temperature in each hour for every day was also recorded (29 ± 2°C; RH $<80\%$). A total number of 750 blind data were collected within a week.

TVS900 (With Direct Skin Temperature Reading)
The system was operated in Metrology Laboratory, Nanyang Technological University, a temperature-controlled environment (23 ± 1°C; RH $<80\%$). There were 30 people that participated as the subjects of the study for three different conditions: normal, after consuming hot drinks, and after running. A 20° lens that is suitable for objects placed at a distance of more than 0.5 m was used. Throughout the temperature-taking session, the scanner was fixed at a distance of 1 m off the subjects. The parameters

setting of the system were: emissivity = 0.98, atmosphere temperature = 30.5°, subject distance = 1 m, transmittance = 0.965, and RH = 0.8. Under normal conditions, body temperatures were taken in three different sites (ears, mouth, and temple) using ear digital (clinical Braun Thermoscan IRT 3520+), mercury, and strip thermometers, respectively. At almost the same time, IR images of front and both sides of the subject's face were also being captured. Under the second condition, each person was to run the same distances of 7×15 m (some people run in the sun without perspiring much). Immediately after they completed the distance required, any sweat on their faces was wiped dry, and three face images (the front and both sides) were recorded for an intervenient time. At the same moment, temperature measurements using contacting devices (digital, mercury,

and strip thermometers) were also taken. The steps in temperature taking under the third condition were performed in a similar manner to that of the running case, except that people were asked to drink a cup of hot tea. The skin surface temperatures (forehead, adjacent to the eyes, temples, and ears) captured in the images were analyzed using the thermal scanner software [10]. The parameters of interest were the average temperature within a small circular pointer from a pointer to a point on specific sites.

Results and Discussion

A data analysis performed on 750 blind samples showed that, in general, the left ear temperature is slightly higher (not > 1 °C) than the right ear (Figure 1). Since the ear temperature resembles brain temperature, it makes sense to measure the left ear temperature for better correlation. The analysis also confirmed that the temperature of a healthy adult human is approximately 36.8 °C, and the temperature of a feverish adult is 37.7 °C or higher.

Fig. 1. Left versus right ear temperatures (°C, based on age group and sex).

Data Analysis with IRTRS (Using External TRS and Color Display Only)

The IRTRS located in a hospital initially had its TRS set to 35.1 °C. This value followed the setting of the IRTRS operation in an air-conditioned environment. Obviously, a different TRS setting should be used for IRTRS operation in a nonair-conditioned environment. An image of a typical feverish staff member taken by IRTRS is shown in Figure 2 (light area of intensity over forehead). The analysis using ImageTool, ImageJ, and Microsoft Excel, however, resulted in a TRS of 35.5 °C to obtain red spot areas that cover 30% of the total face and neck area. The procedure to obtain the TRS temperature threshold consisted of four steps:

1) Ten images of identified feverish staff members were analyzed to extract the three representative parameters for each image. They were the maximum gray value of adjacent (inner corner) of eyes and the average gray values for both blackbody calibrators (as appeared in the upper-left images as two circles, lighter in color, Figures 2 and 3). We extracted the parameters using ImageTool as follows:

• The region of interest (ROI) in the image was chosen by selecting it with a square-shaped cursor. The cursor was placed around the eyes area to obtain the maximum gray value of the adjacent eyes. In the case of obtaining average values of blackbody calibrators, a cursor of the same size was positioned in the middle of the circles. The gray values of both blackbody calibrators captured by the scanner varied in values for every image (due to variation in the operating environment, quality of blackbodies, thermal imagers with different degrees of temperature drift between self correction, uniformity within field of view, minimum detectable temperature difference, error and stability
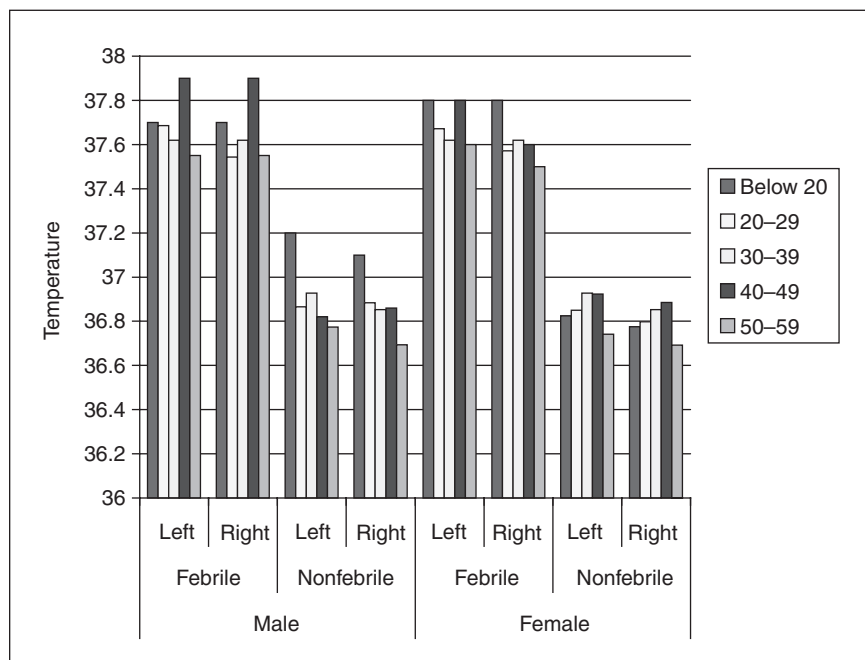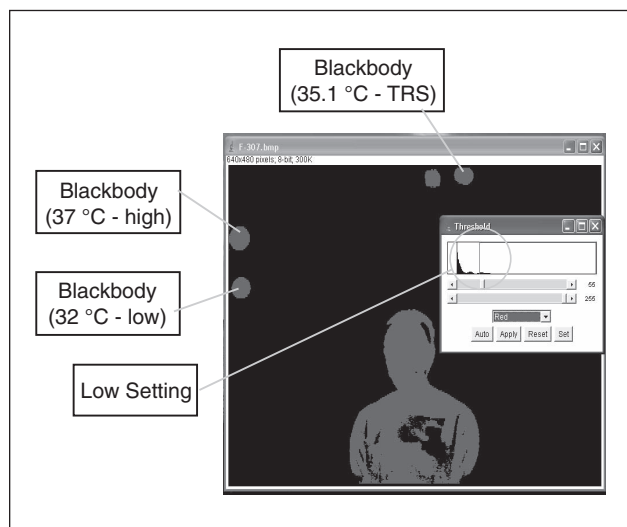

Fig. 2. Image with a low threshold setting value (a feverish staff).

of threshold temperature, distance effect, and detector sizes). Theoretically, these variations should not exist since the blackbody calibrators were expected to emit constant radiation throughout the measurement.

2) The temperature in Celsius scale (°C) was obtained by assuming a linear correlation between its values and the gray values of both blackbody calibrators. As an example, x_1 and y_1 correspond to a blackbody that was set to 32 °C; x_3 and y_3 correspond to a blackbody that was set to 37 °C; and x_2 and y_2 correspond to the adjacent eye area.

- Low gray value, x_1: 70.167
- Low temperature, y_1: 32 °C
- High gray value, x_3: 117.857
- High temperature, y_3: 37 °C
- Maximum gray value, x_2: 129
- Tympanic temperature: 38.1 °C
- Maximum temperature,

$$y_2 = ((x_2 - x_1)/(x_3 - x_1))((y_3 - y_1) + y_1 = 38.168\ °C$$

As expected, tympanic temperature resembled the deep body temperature taken by contact method, whereas y_2 resembled the adjacent eye temperature taken by the noncontact method.

3) Initially, a gray value (x_4), which is also termed *threshold*, was randomly set to obtain red spot areas of 30% of the overall face and neck area. Since the blackbodies' gray values were not the same for every image, the temperature value (y_4) for this specific threshold (x_4) was calculated using the same method as in Step 2.

4) The temperature value (y_4) for every image was set to the same value, and it was converted to the respective gray value again for different images. Several images of feverish and nonfeverish subjects were observed by setting the value to the threshold calculated previously. Next, the red spot areas that appeared

were calculated to check whether they cover up to 30% of the face and neck area of the subject. This step was repeated with the "yes" answer until the desired threshold value was obtained. This value is being used in the operation of IRTRS to help a layman to differentiate conveniently the feverish patients from the normal ones (see Table 1). Figure 3 illustrates a typical distribution of red spot area (in %) as a function of ear temperature. The correlation is rather low due to the small sample size of available febrile cases and because the manual extraction of numeric data is time-consuming for the current Type 1 scanner.

The highest temperature over the front area of face and neck is the area adjacent to the eyes. This finding was obtained by setting a high threshold value for any images. The red spots that remained when a high threshold value was set indicated that the spots had the same temperatures or higher than the corresponding threshold value. In fact, there are quite a few arteries around the eye (the ophthalmic artery is in vicinity to the lacrimal caruncle and it is con-
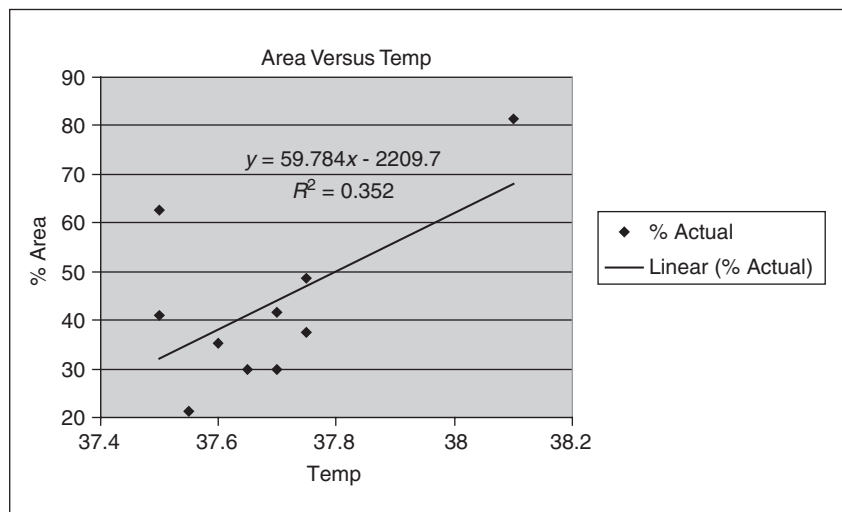

Fig. 3. Area percentage (red spots) versus ear temperature distribution (°C, limited febrile cases).

Table 1. Sample of determining a TRS value (iterative-steps are indicated as 1–6).						
Sample		30% of		% of red spot		Threshold temp
Number	Total Face Area	Face Area	Red Spot Area	over total	Threshold (x)	value (y) °C
421	8560	1712	1815	21.2	119 1	35.5 2
613	5375	1075	2198 5	40.9 6	125.7 4	35.5 3
307	5727	1145.4	4659	81.4	103.5	35.5

nected to the optic nerve) [11]. Thus, a small area of skin near the eyes and nose offers the body core temperature to be measured since the thin skin in this area has the highest amount of light energy, making it a preferred point. With a higher threshold setting, the same image as Figure 2 would clearly indicate the higher temperature adjacent to the eyes (not included here).

Statistical results showed that eye temperatures obtained by IRTRS fluctuated even for the nonfebrile subjects. Although individual variations occur, the inside human body temperature is fairly constant, with small variations over the daily cycle and small variations between individuals. The correlation coefficient between eye (noncontact) and ear temperatures (contact) is about 0.541 (Figure 4; note that many data points overlap operating points for normal subjects). The low correlation may be due to the instability of the camera in capturing images (proven by different gray values for the blackbodies in every image), the changes of the operator experience in temperature screening, standing positions that were not always the same (many of the subjects were in a hurry), the small number of the feverish population, and the method to analyze the data collected. The method to acquire gray values of the blackbodies as described previously involved time-consuming manual interpretation. Thus, accuracy in obtaining the correct values was still greatly dependent on the operator experiences. Figure 5 presents the distribution of contact (ear) and noncontact (eye) temperatures for both normal and febrile subjects. The Pearson Moment Correlation Coefficients (R values) of ear versus eye are 0.224 and 0.3 for normal and febrile subjects, respectively. These values are low, as expected, since we are plotting them separately.

In reality, the body determines a temperature as its so-called set point at any one time during the body temperature regulation [12]. Fever happens if the hypothalamus detects pyrogens and then raises the set point. The time course of a typical fever can be divided into three stages. When the fever begins, the body attempts to raise its temperature, but vasoconstriction occurs to prevent heat loss through the skin. For this reason, some individuals at this stage of fever (at the rising slope and immediately after the fever begins or the falling slope after the fever breaks) will not be detected by the scanner if it is not designed to detect the subject at the plateau of the fever (with her/his high core temperature).

Data Analysis with TVS900 on Subjects with Various Conditions

Reproducibility of both the instrument and physiological assumptions was established by comparing paired left-right readings of the temples and cheeks (not shown here). It is observed that a majority of the data has a very small difference between the left and right readings. In fact, it can be concluded that zero difference was obtained in the highest number of patients.
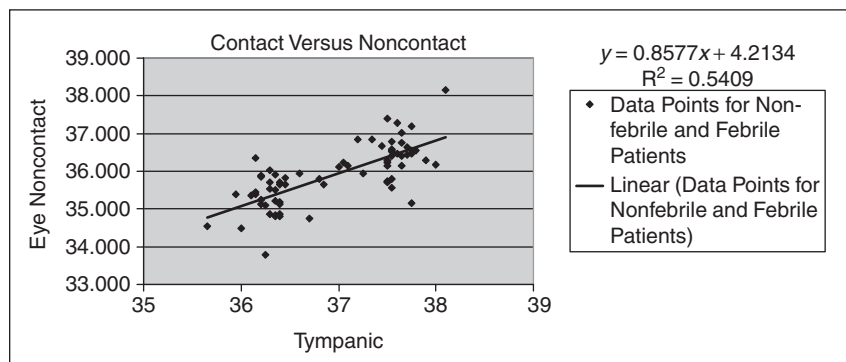
Fig. 4. Linear regression of eye versus ear (tympanic contact) temperature (°C). Note that many data points overlap operating points for the normal subjects.
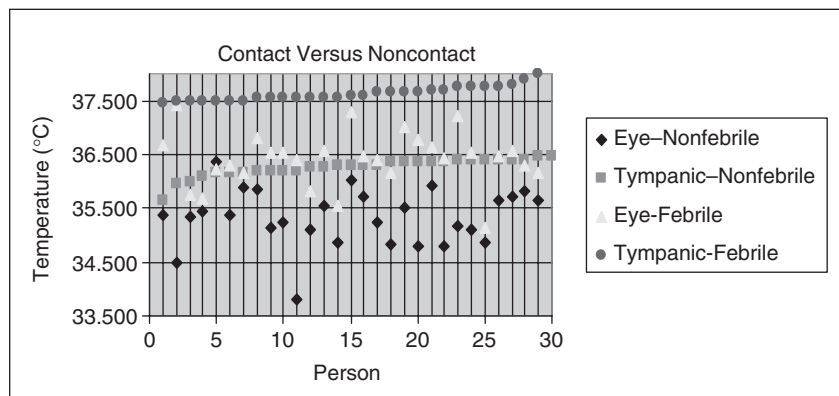
$y = 0.8577x + 4.2134$
$R^2 = 0.5409$

Fig. 5. Graph showing eye and ear temperatures (°C) of febrile and nonfebrile patients (R values are 0.224 and 0.3 for normal and febrile subjects, respectively).

| Table 2. Statistical analysis of significant deviation and standard error.		
Numbers/Site	Temple (Left–Right)	Cheek (Left–Right)
Mean	0.040106952	−0.02513
Standard Error	0.028265764	0.02846
Median	0	0
Mode	0	0
Standard Deviation	0.386528511	0.389181
Sample Variance	0.14940429	0.151462
Kurtosis	1.086850727	2.057879
Skewness	−0.159101714	−0.30164
Range	2.6	3
Minimum	−1.4	−1.5
Maximum	1.2	1.5
Sum	7.5	−4.7
Count	187	187
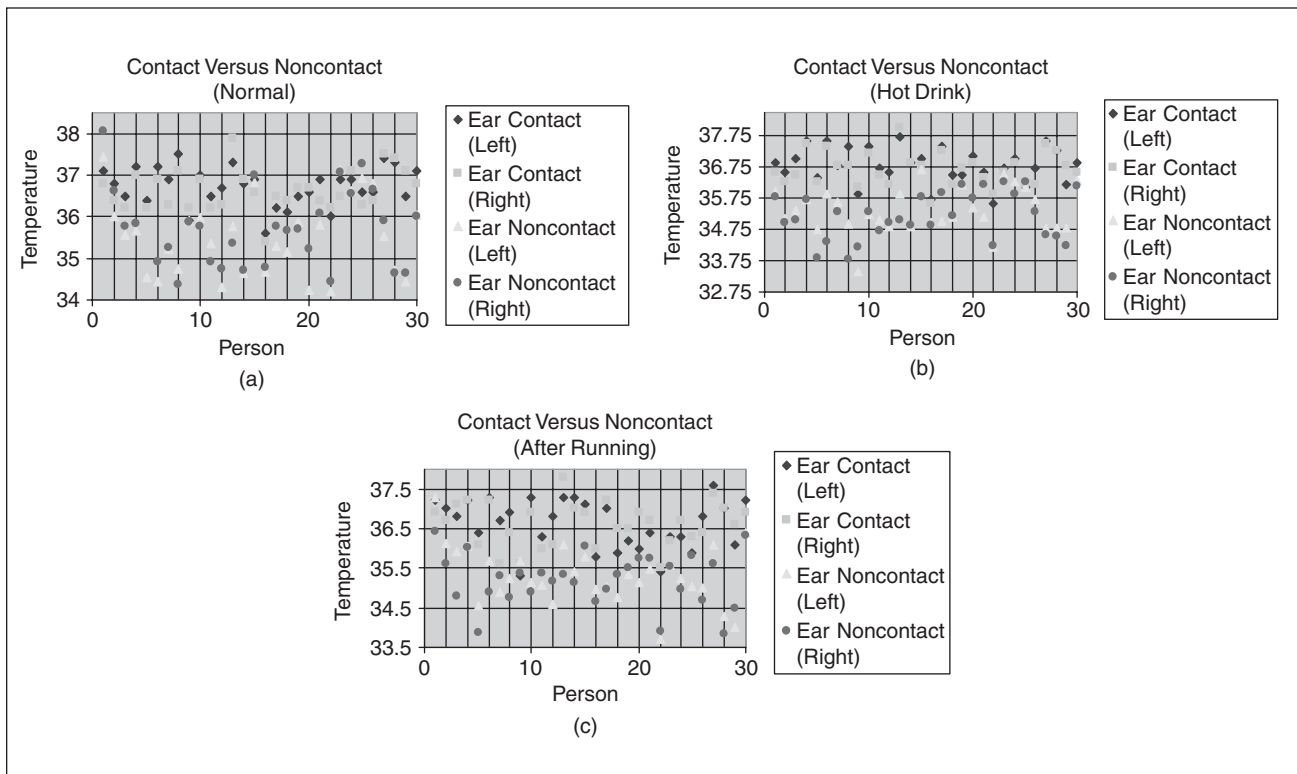
Fig. 6. (a) Normal condition. (b) After a hot drink. (c) After running.

The highest differences between the left and right readings were around ± 0.9 and $\pm 1.5°C$ for the temple and cheek, respectively. These differences are considered low since the number of occurrences with these variations is low. The statistical analysis of significant deviation and standard error from normal distribution is included in Table 2. Therefore, this TVS900 imager can be said to have considerable good reproducibility.

The observation of 30 people's images taken by TVS900 [10] revealed that the most stable and hottest site is the ear area, regardless of the external condition applied (in this case, after running and after consuming a glass of hot tea). Generally, there is not much difference between the left and the right temperatures of both ears and the adjacent eye area. Temperatures of the left and right side temples were slightly scattered for the three conditions. Temperature measurement should not be taken at the forehead since the observation showed that the data fluctuated highly (this observation also exists for eye temperature as in the previous section).

Contact methods, such as mouth temperature measured by mercury thermometer, best resemble deep body temperature, but it is time-consuming and not a practical site during SARS outbreaks. Generally, this temperature is slightly higher than both ear temperatures taken by tympanic thermometer.

The correlation of the ear temperature (contact versus noncontact) at subject conditions specified as normal (resting without extra activity = 0.614), after consuming a hot drink (0.714), and after running 105 m (without perspiring much = 0.787), respectively. Based on statistical results, the ear temperature measured by the contact tympanic ther-

mometer better mimics the actual body temperature. The expected low correlation due to noncontact measurement further confirmed the dynamic balance of heat production; transfer and loss from the various sites of the head in living human beings is a complex process (more so with extra work done by the subject) in which physiologic mechanisms are continuously in action. More analysis with a large sample size is necessary. Figure 6 summarizes ear temperature readings under three different subject conditions.

Conclusions

Accurately mapping the skin surface with body temperatures has been a very important issue for disease diagnostics. Arising from the SARS outbreak in 2003 and the urgent need to screen for febrile individuals through mass screening, IR thermography received more attention in the media worldwide than ever before. Suddenly, IR professionals were supposed to be the heroes that would save the world from this evil disease. Now that the dust has settled, one should ask, what was really the IR contribution? This is a critical and sensitive question; when one goes through some airports lately, it is not uncommon to find that they are still not using IR cameras correctly to detect fever (at least not technically correct, such as focusing issue and distance to spot size ratio >5 mm^2, though it was a political success as far as psychological "warfare" was concerned). Sadly, the general public is still rather uneducated about the most basic physics and methodologies involved in IR thermography. However, it is certain that one can perform a good screening of probable fever cases—if we use the right method and cameras that are thermally stabilized and calibrated.

We have studied the correlation between the facial skin surface and measured tympanic membrane temperature in two types of IR imagers. The results showed that the TVS900 imager Type 2 has good capability in reproducing readings. The noncontact ear temperature was more closely related to contact measured aural (tympanic) reading after running, drinking a hot beverage, and normal conditions. However, the correlation between ear (contact) and eye (noncontact) temperatures taken by IRTRS was relatively lower than what was expected. It is thus essential to give more attention on the device calibration before performing the data collection. The procedures previously suggested allow for more systematic and scientific ways of detecting feverish persons suspected of SARS. The future development of a computerized data processing method is, however, preferable so that less manual work is involved. In the statistical analysis, a setting of of 35.5 °C was found suitable for an IRTRS that is potentially workable.

The results are interesting and will likely be helpful both in designing new IR imagers and in determining how to use them most effectively. The current research application will also remain of interest and be useful for reference by both local and overseas manufacturers of thermal scanners, users, and various government and private establishments. As the elevation of body temperature is a common presenting symptom for many illnesses (including infectious diseases such as SARS). thermal imagers are useful and essential tools for the mass screening of body temperature during public health crises where widespread transmission of infection is a concern at places such as hospitals and cross-border checkpoints.

Acknowledgments

Eddie Y.K. Ng graduated from Cambridge University in 1992. He is an associate professor at the Nanyang Technological University in the School of Mechanical and Aerospace Engineering, Singapore. He is an associate editor for the *Journal of Mechanics in Medicine and Biology* and the *International Journal of Rotating Machinery* and the *Chinese Journal of Medicine* and regional editor for the *Computational Fluid Dynamics Journal.* He has published more than 212 papers in refereed international journals, international conference proceedings, and others. His interest is in computational fluid dynamics, turbomachinery aerodynamics, nanoscale computation, thermal imaging, human physiology, bioinformatics, and biomedical engineering.

Wiryani Muljo graduated from Nanyang Technological University, Singapore, in 2005. She completed the design specialization course from the School of Mechanical and Aerospace Engineering.

B. Stephen Wong is an associate professor and has been a lecturer in Nanyang Technological University, Singapore, for 18 years, mostly with the School of Mechanical and Aerospace Engineering, where he presents course modules and conducts research in nondestructive testing (NDT). Before this, he worked for 13 years in the United Kingdom, conducting research. He has a Ph.D. in physics from the University of Manchester, United Kingdom, and has published more than 40 papers in various journals and conferences, mainly in NDT. He is a member of the Overseas Advisory Panel for the British Institute of NDT for Singapore and is a technical NDT auditor for the Singapore Laboratory Accredition Service.

Address for Correspondence: Eddie Y.K. Ng, School of Mechanical and Aerospace Engineering, College of Engineering, Nanyang Technological University, 50 Nanyang Avenue, Singapore 639798. Phone: +65 6790 4455. Fax: +65 6791 1859. E-mail: mykng@ntu.edu.sg.

References

[1] S.M. Peiris, S.T. Lai, L.L.M. Poon, Y. Guan, L.Y.C. Yam, W. Lim, J. Nicholls, W.K.S. Yee, W.W. Yan, M.T. Cheung, V.C.C. Cheng, K.H. Chan, D.N.C. Tsang, R.W.H. Yung, T.K. Ng, and K.Y. Yuen, "Coronavirus as a possible cause of severe acute respiratory syndrome," *Lancet,* vol. 361, no. 20, pp. 1319–1325, 2003.

[2] T.G. Ksiazek, D. Erdman, C.S. Goldsmith, S.R. Zaki, T. Peret, S. Emery, S. Tong, C. Urbani, J.A. Comer, W. Lim, P.E. Rollin, S.F. Dowell, A.E. Ling, C.D. Humphrey, W.J. Shieh, J. Guarner, C.D. Paddock, P. Rota, B. Fields, J. DeRisi, J.Y. Yang, N. Cox, J.M. Hughes, J.W. LeDuc, W.J. Bellini, and L. J. Anderson, "A novel coronavirus associated with severe acute respiratory syndrome," *New England J. Med.,* vol. 348, no. 20, pp. 1953–1966, 2003.

[3] E.Y.K. Ng and G.J.L. Kaw, "IR scanners as fever monitoring devices: Physics, physiology and clinical accuracy," in *Biomedical Engineering Handbook,* Nicholas Diakides, Ed. CRC Press, 2006, pp. 24.1–24-20.

[4] E.Y.K. Ng, "Is thermal scanner losing its bite in mass screening of fever due to SARS?," *Med. Phys.,* vol. 32, no. 1, pp. 93–97, 2005.

[5] E.Y.K. Ng, G. Kaw, and W.M. Chang, "Analysis of IR thermal imager for mass blind fever screening," *Microvascular Res.,* vol. 68, no. 2, pp. 104–109, 2004.

[6] E.Y.K. Ng and N.M. Sudharsan, "Numerical modelling in conjunction with thermography as an adjunct tool for breast tumour detection," *BMC Cancer, Medline J.,* vol. 4, no. 17, pp. 1–26, 2004.

[7] S.G., Burnay, T.L. Williams, and C.H. Jones, *Application of Thermal Imaging.* England: Adam Hilger, 1988.

[8] E.F.J. Ring and B. Phillips, *Recent Advances in Medical Thermology.* New York: Plenum, 1982.

[9] IRTRS, private communications, Singapore, 2003.

[10] FLIR Systems [Online]. Available: http://www.flir.com (accessed 15 Mar. 2005)

[11] Virtual hospital, *Atlas of Human Anatomy* (Transl.: R.A. Bergman and A.K. Afifi) [Online]. Available: http://www.vh.org/adult/provider/anatomy/atlasofanatomy/plate17/index.html (accessed 11 Mar. 2005)

[12] A.C. Guyton, *Textbook of Medical Physiology*, 10th ed. Philadelphia, PA: Saunders, 2000.

[13] Standards Technical Reference, *Thermal Imagers for Human Temperature Screening Part 1: Requirements and Test Methods*, TR 15-1, Spring Singapore, 2003.

[14] Standards Technical Reference, *Thermal Imagers for Human Temperature Screening Part 2: Users' Implementation Guidelines*, TR 15-2, Spring Singapore, 2004.